REPORT DOCUMENTATION PAGE

Form Approved
OMB No. 0704-0188

1. REPORT DATE *(DD-MM-YYYY)*	**2. REPORT TYPE**	**3. DATES COVERED** *(From - To)*
05/10/2019	Technical Report	

4. TITLE AND SUBTITLE
Investigations and Analyses of LTE Network Cell Tower Deployments and Impact on Path Loss Calculations

5a. CONTRACT NUMBER
W56KGU-18-D-0004-0001

5b. GRANT NUMBER

5c. PROGRAM ELEMENT NUMBER

6. AUTHOR(S)
Carpenter,John M.; Johnson, Jacob K.; Lofquist, Mark A; Hartley, Keith A;

5d. PROJECT NUMBER

5e. TASK NUMBER

5f. WORK UNIT NUMBER

7. PERFORMING ORGANIZATION NAME(S) AND ADDRESS(ES)
The MITRE Corporation
NIST 325 Broadway (MS 670.02)
Boulder, CO 80305-3326

8. PERFORMING ORGANIZATION REPORT NUMBER
PRS-19-1280

9. SPONSORING/MONITORING AGENCY NAME(S) AND ADDRESS(ES)
DoD CIO

10. SPONSOR/MONITOR'S ACRONYM(S)

11. SPONSOR/MONITOR'S REPORT NUMBER(S)

12. DISTRIBUTION/AVAILABILITY STATEMENT
DISTRIBUTION STATEMENT A. Approved for public release: distribution unlimited.

13. SUPPLEMENTARY NOTES

14. ABSTRACT
This paper provides a methodology and results used to estimate eNB cell tower radii and associated path loss for various ground cover morphologies. The research investigated a variety of eNB cell tower datasets, ground cover morphologies, and propagation channel models to determine the sensitivity of results based on the input data. The paper shows there is a statistical difference in results depending on the cell tower location data set, ground cover morphology classification, and propagation model used. To aid the National Advanced Spectrum and Communications Test Network (NASCTN) an understanding of real-world LTE network path loss must be considered.

15. SUBJECT TERMS
Communications Services; Wireless Communications; mobile broadband3G; LTE network; mobile communications; 4G; cellular networks; Long-Term Evolution; telecommunications;

16. SECURITY CLASSIFICATION OF:			**17. LIMITATION OF ABSTRACT**	**18. NUMBER OF PAGES**	**19a. NAME OF RESPONSIBLE PERSON**
a. REPORT	**b. ABSTRACT**	**c. THIS PAGE**			Susan Carpenito
				43	**19b. TELEPHONE NUMBER** *(Include area code)* 781-271-7646

Investigations and Analyses of LTE Network Cell Tower Deployments and Impact on Path Loss Calculations

John Carpenter
Jacob Johnson
Mark Lofquist
Keith A. Hartley

Sponsor: DoD CIO and TRMC
Department No.: P612
Contract No.: W56KGU-18-D-0004-0001
Project No.: 0719C60D and 0719D110-BA

Document No: MP190327
Boulder, CO

MITRE

ABSTRACT

The long-term evolution (LTE) cellular standard has become a ubiquitous communications protocol for commercial mobile broadband and communication services. The LTE protocol was designed to outperform its 3rd generation (3G) predecessors such as universal mobile telecommunications system (UMTS), global system for mobile communications (GSM) and code division multiple access (CDMA). Design goals of LTE also known as 4th generation (4G) systems are to increase downlink and uplink data rates, provide scalable bandwidth, improve radiometric efficiency, include an all internet protocol (IP) network, and support many user types.

The federal government has undertaken several initiatives to open up federal spectrum for commercial use and share use with commercial and federal services to satisfy the increasing requests for more spectrum to expand LTE services. One of those areas is in the advanced wireless services 3 (AWS-3) bands (i.e., 1695-1710 MHz, 1755-1780 MHz, and 2155-2180 MHz). Initially, federal and early commercial entrants will be sharing the 1755-1780 MHz band. The Defense Spectrum Organization (DSO) sponsored a spectrum sharing project executed by the National Advanced Spectrum and Communications Test Network (NASCTN). The NASCTN project seeks to perform rigorous tests to determine the factors that have the biggest effect on LTE user equipment (UE) behavior with the goal to provide statistically significant data for DSO to improve their decision-making process.

To aid the NASCTN project, an understanding of real-world LTE network path loss must be considered. Quantifying LTE communications network performance requires an understanding of network sizes, antenna heights, and the ground cover that the network is expected to operate in and how that ground cover effects the ability of LTE radiowave signals to propagate.

This paper provides a methodology and results used to estimate eNB cell tower radii and associated path loss for various ground cover morphologies. The research investigated a variety of eNB cell tower datasets, ground cover morphologies, and propagation channel models to determine the sensitivity of results based on the input data.

The paper shows there is a statistical difference in results depending on the cell tower location data set, ground cover morphology classification, and propagation model used.

This page intentionally left blank.

Table of Contents

List of Figures

List of Tables

Introduction

As part of the Characterizing User Equipment Emissions project sponsored by the Defense Spectrum Organization (DSO), the National Advanced Spectrum and Communications Test Network (NASCTN) assembled a test for measuring long-term evolution (LTE) user equipment (UE) behavior over a variety of LTE network settings and (simulated) operational conditions in the advanced wireless services 3 (AWS-3) band, with emphasis on 1755–1780 MHz. NASCTN's goal is to determine the factors that influence LTE UE emissions. The testbed for this measurement campaign is operated by NASCTN staff and located in the Boulder Laboratories located on the Department of Commerce campus in Boulder, CO.

NASCTN requires information on LTE uplink and downlink path loss for its testbed; this paper responds to that need. The paper analyzes deployment data for heterogeneous sets of cell towers (referred to as base stations, enhanced node B, or eNB) from three different sources: proprietary cell site deployment data from a national broadband commercial carrier, a commercial cell tower database[1], and a set of crowd-sourced data [2]. The first data source catalogs a carrier-specific macro-cell eNB placement; [1] contains reported tower sites from a cell tower provider supporting multiple wireless carriers, and [2] encompasses cell tower locations using UE self-reported position and LTE received power values. The paper compares these data sets and categorizes the data to report and analyze encountered morphologies (such as urban, rural, suburban) and correlates these deployment details to cell site spacing in kilometers (km), network size, and estimations of path loss in decibels (dB). The output of this methodology outlines the expected distances (cell radii) and approximate cell edge path loss values experienced by LTE cell towers in various operational conditions, such as in a typical urban or rural cell.

The MITRE researchers used eNB morphology categorization techniques based on population data and land cover databases. Each categorization technique was applied to the three cell tower location data sets. Figure 1 shows the analysis technique.

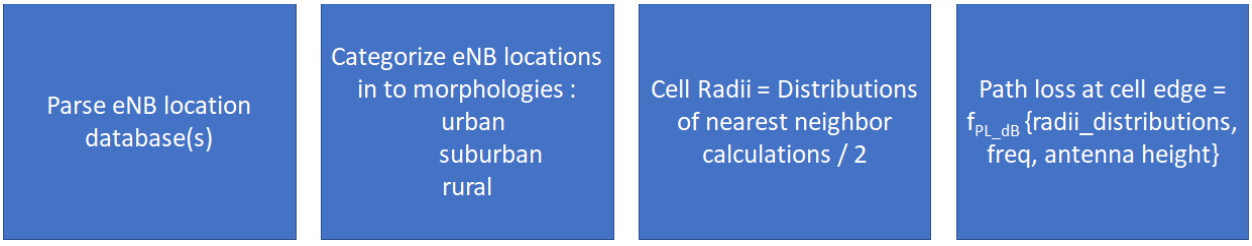

Figure 1. Steps in the Analysis

eNB Cell Tower Location Data Sets

The MITRE team investigated three different data sources of eNB cell tower placements to identify cell tower spacing (and therefore cell radii). The accuracy of cell tower placement varies among the different data sets. In order to calculate the effects of the various cell tower location errors, the team analyzed each data set for comparison.

As noted above, the first data set stems from a member of the wireless provider community operating within the United States.[1] The second data set [1] is provided freely online by a manufacturer of cell towers (American Tower), and the third data set [2] is drawn from a crowd-sourced cell tower database called OpenCellID. The team used these data sets to give a representative sample of eNB cell towers across the United States.

Data Set 1: LTE Network Service Provider

The data set provided to NASCTN encompasses a large amount of information that catalogs eNB cell tower locations across various densities in population, although it is not inclusive of the entire United States. The data set covers just over 14,000 cell tower points in the United States. Research in 2017 estimated there are 215,000 eNB cell tower sites across the continental United States (CONUS) [3]. Despite its limited quantity, the data set spans a large number of land cover types and gives data across major regions in the United States. For the purposes of developing the methodology and subsequent statistical analysis, this research used data on the coordinates of current and future macro-cell eNB cell tower deployments and their anticipated or deployed antenna heights. The path loss calculations use only macro cells in order to mirror the NASCTN experiment.

Data Set 2: American Tower Location Data

The second data set was produced by American Tower and is accessible after registration [1]. American Tower maintains and builds towers on which carriers can lease space for their eNB equipment. American Tower provides tower deployment information publicly accessible on the internet. The data set contains the geospatial coordinates of each tower the company maintains as well as the maximum tower height. However, the data set does not reveal which telecommunications company or frequency bands are on each specific tower.

Data Set 3: Crowd-sourced Data from OpenCellID

The third data set is taken from an open crowd-sourced database called OpenCellID[2] and is accessible after registration [2]. The database receives user submissions from smartphone applications or GET requests via the OpenCellID application program interface (API). Each row in the database allows users to find the county code, mobile network code, approximate coordinates of the tower pinged, the range (distance) between the UE and the cell tower, and the number of UEs that have reported connecting to this tower. Importantly for this research, the data does not include tower height and eNB type for each cell tower.

[1] In the United States, cell service providers treat their eNB cell tower site locations as proprietary information. As a trusted agent to this data source, MITRE does not identify the LTE service provider.

[2] The OpenCellID Project is licensed under a Creative Commons Attribution-ShareAlike 4.0 International License.

Since the exact coordinates of the cell tower are unknown, this data set is the least accurate of the three sources, but was used in the research because it covers the largest area of the United States and could be used to show the "best case" path loss due to the large spatial coverage of the data points. OpenCellID provides data not only on LTE cell locations but also on GSM, CDMA, and UMTS. After thorough examination of this data set, the MITRE team concluded that the research could not use the OpenCellID data because it did not distinguish between the different major wireless carriers (e.g., Verizon, AT&T).

Conclusion

While each dataset has limitations, the LTE service provider dataset gives the best representation of cell tower placement in comparison to the American Tower and OpenCellID datasets because it contains locations of a single service provider's cell towers, at one frequency band, and respective antenna heights. Therefore, the analysis in this paper uses the LTE service provider's data only.

Estimation of eNB Cell Tower Site Spacing

The cell radius must be calculated to determine the path loss of a tower. This paper uses the term "cell radius" to describe the radius of an assumed circular signal coverage area of a cell tower, disregarding antenna patterns or variations due to terrain. Path loss calculations can vary significantly depending on a given channel model's sensitivity to propagation distance. For example, the Friis propagation model [4] has a straightforward dependency of $\frac{1}{r2}$, whereas the Extended Hata model [5] has losses associated with building clutter and was derived from drive testing through various population centers. Propagation models are highly dependent on distance. In practice, antenna patterns from an eNB are very complex to model. It should be noted that the methodology described in this section assumes that all cell towers have a circular radius. The calculations in this paper assume that coverage from the same provider does not overlap (on average, there is equal likelihood a user would attach to either eNB in an overlapping coverage scenario).

In this paper, the cell radius of a tower is assumed to reach only as far as the nearest neighbor's cell radius. For example, if two towers are one kilometer apart, the cell radius of each tower is 500 meters (no overlapping was considered in this paper). This is known as a nearest neighbor calculation. The researchers developed a Python script to efficiently determine the nearest neighbor of thousands of towers. Once the nearest neighbor is known for each tower, the distance between each tower is divided by two. The Python script utilizes Sci-Kit's ball tree [6] package to sort the towers and calculate the distances between them. Algorithm 1, the pseudocode for ball tree, is shown in Figure 2 and describes the process of calculating cell radii. After the points are sorted into the ball tree, the tree is queried for the distance of the closet points. Each radius calculation uses the Haversine equation (Equation 1) [7] to accurately determine the distances between points. The distance is divided by two and is saved as a comma-separated values (CSV) file with each latitude and longitude point, the radius in kilometers (km), and the height of the tower in meters (m), if given by the data set. If the data set does not include the height, as in the crowd-sourced and American Tower data files, the researchers used an average height for all towers. The average height of the provider data set is approximately 40 m, while the median is approximately 34 m. The researchers used the Haversine formula for this study because they calculated the distance between two points over the Earth (this assumes the Earth is a perfect sphere). Equation 1 shows the Haversine formula solved for distance.

$$d = 2r \arcsin\left(\sqrt{sin^2\left(\frac{\varphi_2 - \varphi_2}{2}\right) + \cos(\varphi_1)\cos(\varphi_2)\, sin^2\left(\frac{\lambda_2 - \lambda_1}{2}\right)}\right) \qquad (1)$$

where:

φ_1, φ_2 = latitude of points 1 and 2

λ_1 = longitude of points 1 and 2

d = distance (km)

r = Earth's radius (km).

The ball tree algorithm [8] is useful for computing the nearest neighbor for each cell tower. A ball tree is a binary tree in which each level of the tree contains a ball that encircles a

subset of coordinates. On the first level of the tree, every point is contained in a single ball. The second level of the tree splits the ball into two and the algorithm determines which coordinates are closest to the centroid of each ball. A tower's coordinates are assigned to a single ball. As the height of the tree increases, the number of balls increases and the number of coordinates contained within each ball decreases. After the algorithm terminates, the Haversine distance between a subset of the coordinates contained within each ball is calculated.

The algorithm is efficient because the resource-intensive distance calculation is only performed for coordinates within a single ball. The algorithm can be adjusted to include more coordinates within each ball or produce more balls with fewer coordinates. If there are too many coordinates within a ball, then the Haversine formula must be used for each coordinate in the ball. If there are only two coordinates within each ball, the algorithm takes longer to run but the Haversine formula is only used once. This creates a tradeoff between the number of balls and the number of times the Haversine formula is calculated. Sci-Kit's package determines the optimal number of balls and Haversine calculations through training data and artificial intelligence [9]. The MITRE researchers used the algorithm in Figure 2 to produce the cell tower radius graphs. The pseudocode for this algorithm was developed by the Department of Computer Science at Cornell University and presented in a series of lecture slides [8]. This pseudocode gives a general run-through of how the recursive algorithm works.

Algorithm 1 Balltree in Pseudo-code

procedure BALLTREE(S, k)
  if $|S| < k$ **then** stop **end if** ▷ Return leaf containing S
  pick $x_0 \in S$ uniformly at random
  pick $x_1 = \text{argmax}_{x \in S}\ d(x_0, x)$
  pick $x_2 = \text{argmax}_{x \in S}\ d(x_1, x)$
  $\forall i = 1 \ldots |S|, z_i = (x_1 - x_2)^T x_i$ ← project data onto $(x_1 - x_2)$
  $m = \text{median}(z_1, \cdots, z_{|S|})$
  $S_L = \{x \in S : z_i < m\}$
  $S_R = \{x \in S : z_i \geq m\}$
  Return tree:
  – center $c = \text{mean}(S)$
  – radius $r = \max_{x \in S} d(x, c)$
  – children: Balltree(S_L, k) and Balltree(S_R, k)
end procedure

Figure 2. Algorithm 1 Ball Tree in Pseudocode [8]

Data Categorization Techniques

Technique A: Census Data

Introduction

A signal's path loss is highly dependent upon the clutter found between the UE and the eNB. The set of morphologies (urban, suburban, and rural) or expected clutter types around an eNB cell tower can be established by using the ZIP code tabulation area (ZCTA) data set. The Census Bureau uses ZCTAs over typical ZIP codes because the boundaries of ZIP codes change as mail routes evolve, while ZCTA boundaries only change as the population changes [10]. The ZCTA data set contains polygons outlining each ZCTA. As an example, Figure 3 shows an overview of these polygons for Manhattan.

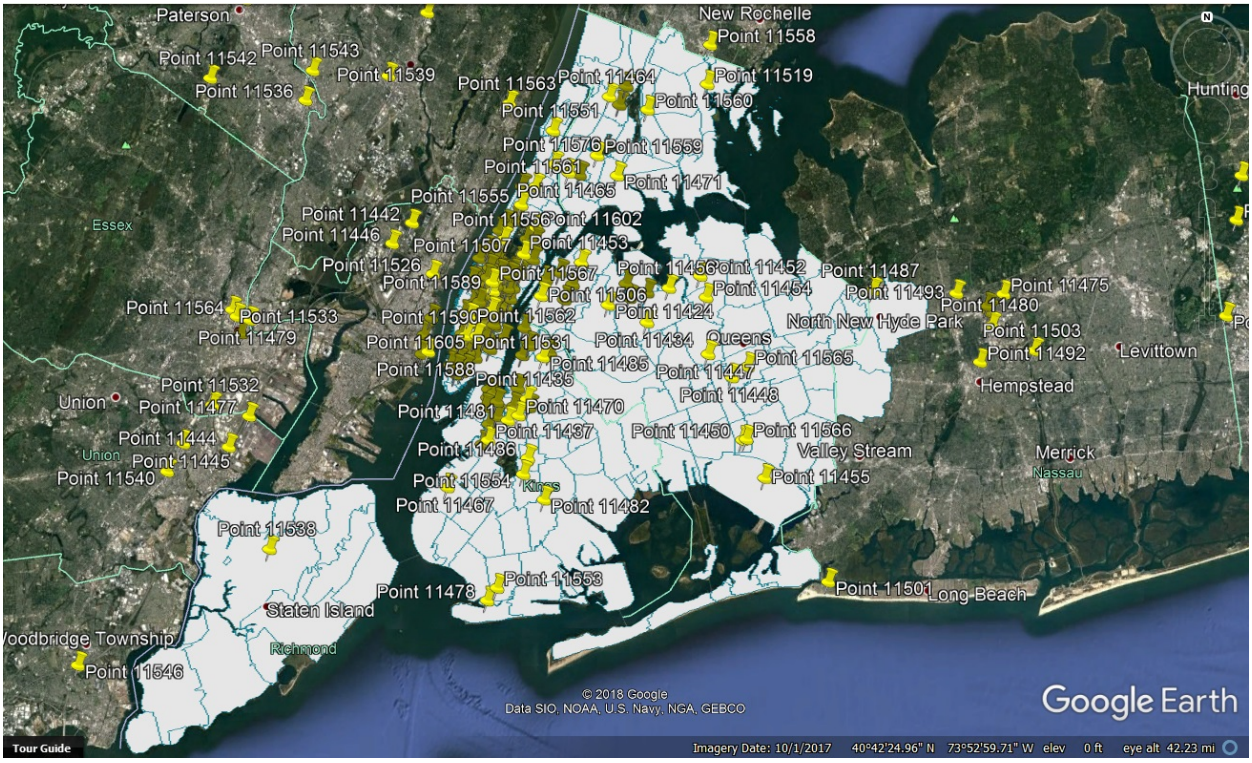

Figure 3. Overview of Reported Cell Tower Locations in ZCTA Polygons in Manhattan

The 2010 Census contains population information for each ZCTA, which is mapped to the polygon data to establish a morphology for each ZCTA [11]. The file for this data is called the Urban to ZCTA Relationship CSV file. Within this file, there are columns for each ZCTA in United States. In each row are two columns that contain the ZCTA and the morphology classification. If a ZCTA is in an urbanized area, the column specifies if the area is an urban cluster (suburban) area or an urban area. If the ZCTA is not in an urbanized area, the row states "Not in a 2010 urban area," which means the area is rural.

The Census Bureau calculates the percentage of a population living within rural, suburban, and urban areas inside a ZCTA and uses the morphology with the majority percentage of the total population of a ZCTA as the morphology for the entire ZCTA. These morphologies allowed the researchers to begin estimating path loss values given a propagation channel

model. The ZCTA method for classifying morphologies sets an entire polygon as a single morphology. This is useful but could contain edge cases. For example, a tower could be in a suburban ZCTA, but the tower's exact location is on a farm in a rural subsection of the area. Therefore, the Census and ZCTA method may not reflect the exact morphology of a tower because a tower may only cover a small subsection of a significantly larger ZCTA. To more accurately estimate the morphology of a tower, only the area within a tower's cell radius should be classified as the morphology. In order to accomplish this, spectral [12] imaging can be used to classify land within a small area.

Technique

The ZCTAs are organized into one of three morphologies: urban, suburban, and rural. The research team used the ball tree algorithm shown in Figure 2 on each of the three data sets for each of the ZCTA morphologies to determine the mean cell radii for each morphology.

Cell Site Spacing Results (in km)

Table 1 shows the results of calculating the mean cell radii using the Census data and ZCTA data categorization (i.e., urban, suburban, rural).

Table 1. Median Cell Radii Using the Ball Tree Algorithm

	Cell Radii Mean (km)		
Type	**Rural**	**Suburban**	**Urban**
Census Data	8.52	3.34	1.6

Limitations

The limitations of using the Census data and ZCTA for data categorization include:

- ZCTA overly generalizes large portions of land. There could be very large variations in propagation characteristics within a single ZCTA.
- Census data and ZCTA do not take into account buildings, foliage, or other natural/man-made obstacles that impact radio propagation.
- ZCTA categorizes population based on where people reside, not where they travel or work. Therefore, the ZCTA regions may not accurately represent cell phone usage. For example, many travelers on a highway traverse areas that have no residents but require cell service coverage.

Summary

ZCTA is a method used to categorize population area into morphologies using Census data. However, it has significant limitations when trying to use the morphologies to accurately categorize data. For this reason, the researchers identified an alternate approach, described in the next section, to allow comparison of results.

Technique B: Land Cover Data

Introduction

The Multi-Resolution Land Characteristic Consortium generates land cover data from its national land cover database (NLCD) [13]. The land use is classified by 30mx30m squares across the entire country. The number of 30m x 30m squares across the entire United States is significantly greater than the number of ZCTAs, allowing for morphology classification at finer resolution. The researchers used the generalized coverage area of a cell or cell radius to cut an area out of the data. Each pixel within the cell radius corresponds to a specific land cover type as shown in Table 2, which lists the corresponding NLCD ID values for the land cover types. The land cover types are used in the morphology calculations in Figure 4.

Table 2. NLCD ID Values for Land Cover Types

NLCD Pixel ID	Land Cover Type
11	Water
12	Ice/Snow
31	Barren
71	Grassland
95	Emergent Herbaceous Wetlands
52	Shrub/Scrub
81	Pasture/Hay
82	Cultivated Crops
90	Woody Wetlands
41	Deciduous Forest
42	Evergreen Forest
43	Mixed Forest
21	Developed, Open Space
22	Developed, Low Intensity
23	Developed, Medium Intensity
24	Developed, High Intensity

The researchers then calculated the percentages of each land cover type in a given cell and inserted them into an algorithm developed by the Defense Information Systems Agency (DISA). The percentage of land cover pixels found within the cell tower radius determines the corresponding morphology. The inequalities for the seven morphologies are shown in Figure 4, which returns the cell's morphology. Since the NLCD contains far more data than ZCTA on classifying land use, DISA's algorithm returns one of seven possible morphologies:

- Dense urban
- Urban
- Suburban
- Forested
- Rural
- Rural forested

- Barren

Dense Urban:

$$NLCD\ 24 + NLCD\ 23 \geq 0.5\ \textbf{\textit{and}}\ NLCD\ 24 \geq 0.25$$

Urban:

$$NLCD\ 24 + NLCD\ 23 + NLCD\ 22 \geq 0.5\ \textbf{\textit{and}}\ NLCD\ 23 \geq 0.25$$

Suburban:

$$NLCD\ 24 + NLCD\ 23 + NLCD\ 22 + NLCD\ 21 \geq 0.15$$

Suburban Forested:

$$NLCD\ 24 + NLCD\ 23 + NLCD\ 22 + NLCD\ 21 \geq 0.15\ \textbf{\textit{and}}$$
$$NLCD\ 43 + NLCD\ 42 + NLCD\ 41 + NLCD\ 90 \geq 0.05$$

Barren:

$$NLCD\ 11 + NLCD\ 12 + NLCD\ 31 + NLCD\ 71 + NLCD\ 95 \geq 0.9$$

Rural Forested:

$$NLCD\ 43 + NLCD\ 42 + NLCD\ 41 + NLCD\ 90 \geq 0.5$$

Rural:

Anything else

Figure 4. NLCD Equations

Using this method, the researchers obtained a far more granular representation of cell usage and propagation characteristics. For example, Figure 5 shows the land cover areas for Georgetown in Washington, D.C. This highlights the increased resolution NLCD provides, as multiple NLCD areas are shown in what ZCTA would classify only as urban or suburban. Overlaying nominal cell radii on the land use data provides a more realistic understanding of the expected propagation. Figure 6 shows the land cover areas for the entire United States of America (USA) [14] and Figure 7 provides the legend to interpret colors for each of the land coverage types used within the NLCD [15].

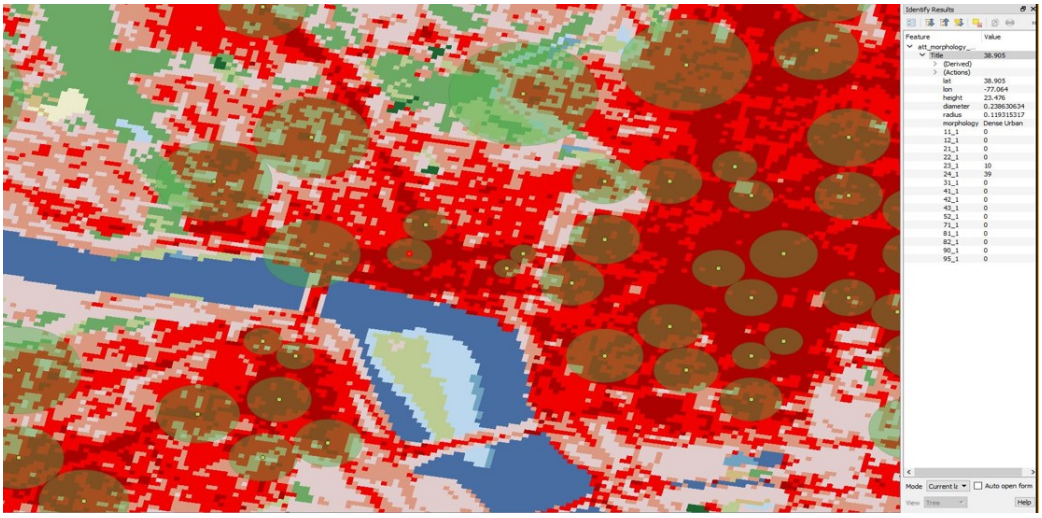

Figure 5. Snapshot of Georgetown in Washington, DC, Using the National Land Cover Database in QGIS

Figure 6. Snapshot of the National Land Cover Database

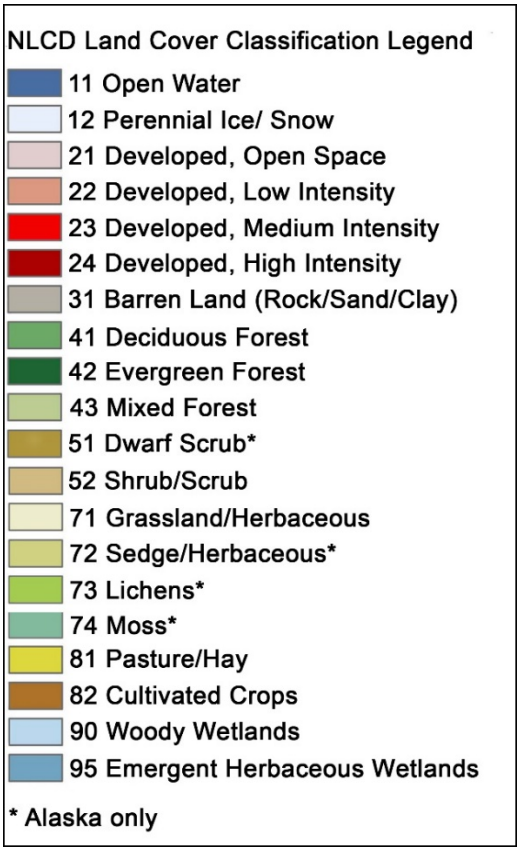

Figure 7. Legend of Pixel Values Pertaining to the National Land Cover Database

Technique

The same ball tree algorithm technique described in Figure 2 was applied to the NLCD data. However, since the NLCD data has seven categories while ZCTA only used three, several categories are lost.

Cell Site Spacing Results (in km)

Table 3 shows the results of comparing the three categories that match between ZCTA and NLCD. This clearly shows a difference in results, most strikingly for the rural category, by using different data categorization techniques. Some of this difference stems from the loss of NLCD data that has more categories than ZCTA.

Table 3. Mean Cell Radii Using the Ball Tree Algorithm

	Cell Radii Mean (km)		
Type	**Rural**	**Suburban**	**Urban**
Census Data	8.52	3.34	1.6
NLCD	3.16	1.73	1.03

Due to the greater resolution and granularity, the NLCD categorization techniques can extend beyond the three morphologies provided by the Census data. Table 4 shows the breakout of cell tower and cell radii from all seven NLCD categories. Note that the total number of towers is 14,038, which is equal to the total number of towers in the provider data set.

Table 4. Number of Towers for Each Morphology and Median Radius Using NLCD-based Calculations

	NLCD	
Morphology	**Tower Counts**	**Cell Radius Mean (km)**
Rural	2,329	3.25
Rural Forested	1,968	1.81
Suburban	1,738	1.59
Urban	2,804	1.09
Dense Urban	1.863	0.93
Suburban Forested	3.266	3.09
Barren	70	2.30
Total	14,038	-

Limitations

While the NLCD provides more resolution and granularity than ZCTA, limitations of this method include:

- The increased categories do not easily align with propagation models. For example, the Extended Hata-Okumura model only considers three clutter categories (suburban, urban, and rural).
- Increased categories do not align with past studies, which complicates making comparisons/decisions.

- Morphology selection is based on pixel count proportion found inside the cell tower radius. Changes to the set of inequalities (see Figure 4) will ultimately change the morphology for each cell tower, which in turn will affect the path loss distribution.

Summary

This analysis shows that NLCD provides a more granular view of land use than Census data, which in turn should provide a more realistic understanding of cell radii and propagation characteristics. The drawback of this technique is the difficulty of using it with propagation models that do not take advantage of the increased resolution of land use for propagation calculations.

Conclusion

The following set of figures compares the data sorting method (Census-based versus NLCD-based) for the three morphologies. Figure 8, Figure 9, and Figure 10 are quantile-quantile plots. If the slope of the blue points is linear (following the red extrapolation line) then the distribution of the Census and NLCD radius data sets is the same. The rural plot, Figure 8, has the most linear shape and shows that the two data sets are comparable over a few quantiles. The lack of linearity in the suburban and urban plots, Figure 9 and Figure 10, demonstrates these sorting methods are very different. Since the eNBs are grouped into different categories, the distribution of the distances will be shaped differently. Different distance distributions will lead to different path loss calculations. Therefore, the path loss for each morphology is not expected to share the same distribution due to the different sorting methods.

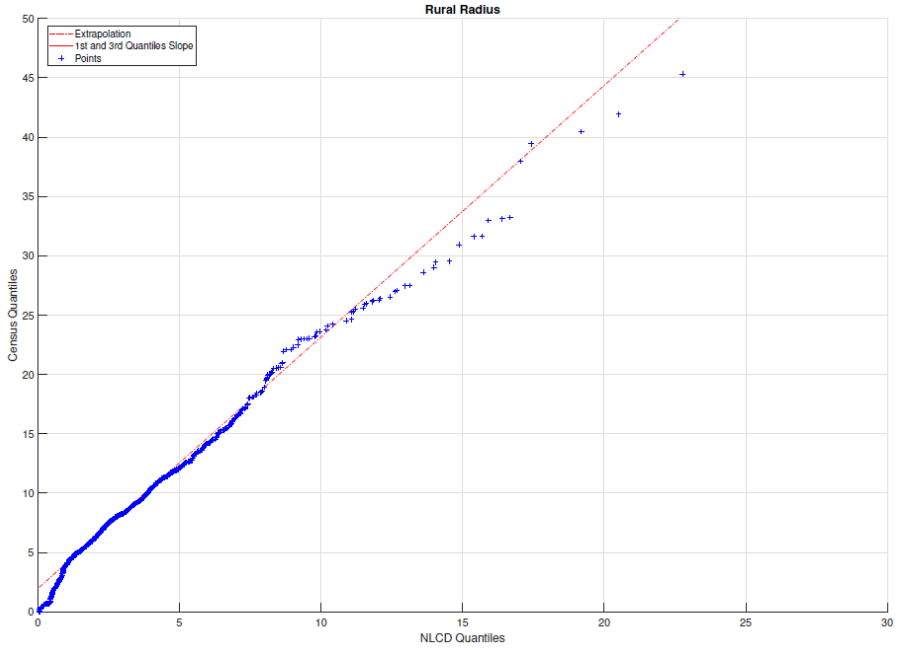

Figure 8. Quantile-Quantile Chart Comparing the Rural Census Radius and the Rural NLCD Radius Distributions

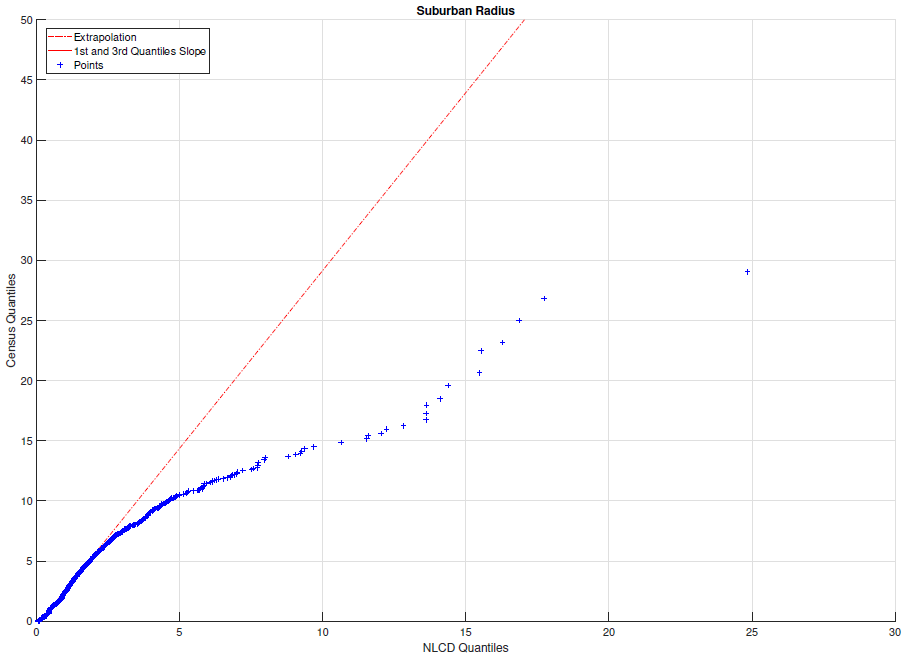

Figure 9. Quantile-Quantile Chart Comparing the Suburban Census Radius and Suburban NLCD Radius Calculations

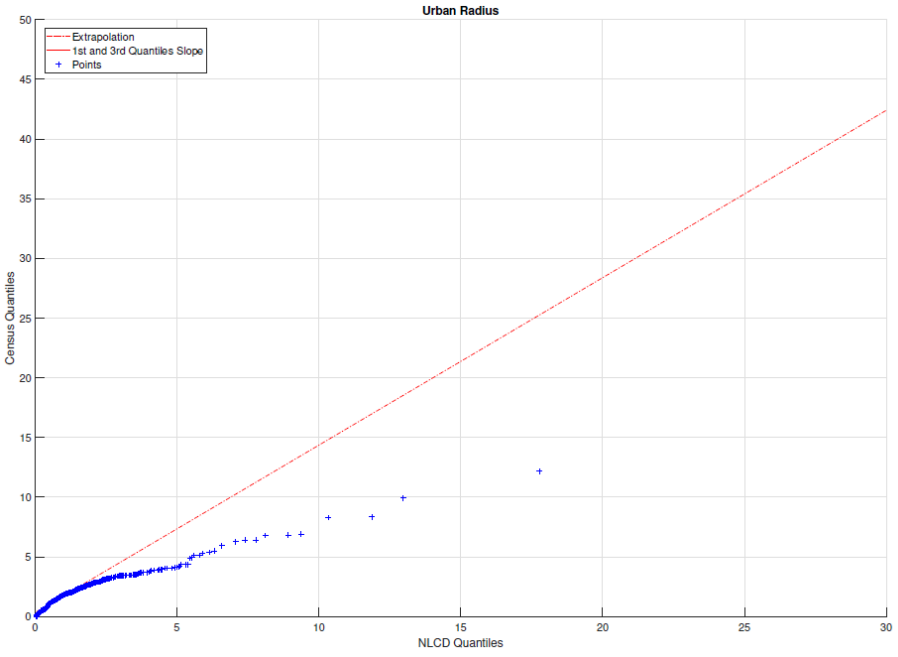

Figure 10. Quantile-Quantile Chart Comparing the Urban Census Radius and Urban NLCD Radius Calculations

Propagation Models

The researchers used three different models in determining path loss from the cell tower radius distributions. The models have varying levels of realism, accuracy, limitations, and input variables.

Friis Free-Space Model

Functionality

The first model considered in this paper is the Friis model [4], commonly referred to as the free space model. The free space model is a direct line-of-sight model and only factors in the radius of each cell. This model works well in areas dominated by direct line-of-sight propagation. When used to calculate the path loss of other environments, such as suburban and urban, the free space model consistently underestimates the path loss of eNB cell tower emissions, since the cell radii are small and thus closer together. As a result, the free space model does not reflect real-world conditions. The free space equation is shown in Equation 2:

$$L = 20log_{10}\frac{(4\pi R)}{\lambda} \quad (2)$$

where:

L = Path Loss (dB)

R = Distance between antennas (m)

λ = wavelength (m)

Limitations

Limitations of the Friis model include:

- Consistently underestimates propagation loss because it assumes line of sight.
- Does not take into account multipath or ground clutter loss from foliage, buildings, clutter, etc.

Conclusion

The free space model serves as a reasonable starting point and is often used to establish best-case propagation limits, considering it does not factor in propagation through terrain or obstacles. For the purposes of this study, the researchers sought a model with more realistic real-world propagation characteristics.

Hata-Okumura

How It Works

The second model considered in this paper is the Hata-Okumura model [16]. This model offers additional loss factors accounting for various building densities. Unlike the free space model, the Hata-Okumura model uses different equations for rural, suburban, and urban

environments, each of which considers base station height and UE height (the researchers assume the average UE height is 1.5m). However, the model has several constraints (e.g., distance, frequency).

Equation 3 shows the Hata-Okumura propagation equation for an urban morphology with scaling factors for small and medium sized urban cities shown in Equation 4 and for large urban cities shown in Equation 5.

For urban environments:

$$L_U = 69.55 + 26.16log_{10}(f) - 13.82log_{10}(h_b) - C_H + (44.9 - 6.55log_{10}(h_b))log_{10}(d) \quad (3)$$

where:

L_U = Path loss in urban areas (dB)

h_B = Height of base station antenna (m)

h_M = Height of mobile antenna (m)

f = Frequency of transmission (MHz)

C_H = Antenna height correction factor (dB)

d = Distance between the base and mobile stations (km).

For small or medium-sized urban cities:

$$C_H = (1.1log_{10}(f) - 0.7)h_M - (1.56log_{10}(f) - 0.8) \quad (4)$$

For large urban cities:

$$C_H = \begin{cases} 8.29(log_{10}(1.54h_M))^2 - 1.1, if\ 150 \leq f \leq 200 \\ 3.2(log_{10}(11.75h_M))^2 - 4.97, if\ 200 \leq f \leq 1500 \end{cases} \quad (5)$$

Equation 6 shows the Hata-Okumura propagation equation for a suburban morphology.

For suburban environments:

$$L_{SU} = L_U - 2\left(log_{10}\left(\frac{f}{28}\right)\right)^2 - 5.4 \quad (6)$$

where:

L_{SU} = Path loss in suburban areas (dB)

L_U = Average path loss from a small city (dB).

Equation 7 shows the Hata-Okumura propagation equation for a rural morphology.

For rural environments:

$$L_O = L_U - 4.78\left(log_{10}(f)^2 + 18.33log_{10}(f)\right) - 40.98 \quad (7)$$

where:

L_O = Path loss in open area (dB)

L_U = Average path loss from a small city (dB).

Limitations

The Hata-Okumura model represents an improvement over the Free Space model, but has several limitations, including:

- It is limited to three morphologies (i.e., urban, suburban, rural), and cannot take into account new morphologies from NLCD.
- Propagation effects are based on outdated measurements.
- Model was not designed for higher frequencies often used by cell services (model designed for $150\ MHz \leq f \leq 1500\ MHz$).
- eNB cell tower height must be between 30 and 200 m.
- UE height must be between 1 and 10 m.
- Cell radii must be between 1 and 20 km.

Conclusion

Hata-Okumura is based on drive testing measurement and includes additional loss factors for urban, suburban, and rural clutter categories. This categorization of morphologies is a better representation over free space, but still contains many significant limitations such as cell radii between 1 and 10 km. The Hata-Okumura model should be extended to take into account smaller distances and higher frequencies and thus offer a potentially more realistic model for this research.

Extended Hata-Okumura

How It Works

The third model considered in this paper is the Extended Hata-Okumura model, which addresses some of the limitations of the Hata-Okumura model. The Extended Hata-Okumura model applies to frequencies from $1500\ MHz \leq f \leq 2000\ MHz$ and accounts for much smaller cell radii. The model includes three clutter loss factors for urban, suburban, and rural morphologies, which are shown in Equations 8 through 12.

Arguments for the Extended Hata-Okumura [5] equations are:

L =Median path loss (dB)

f = Frequency of transmission (MHz)

H_B = Base station antenna effective height (m)

d = Link distance (cell tower radii for the purposes of this research) (km)

H_m = Mobile station antenna effective height (m)

$a(H_m)$ = Mobile station antenna height correction factor for urban areas (dB)

where:

$$a(H_m) = (1.1\log(f) = 0.7)\min(10, H_M) - (1.56\log(f) - 0.8) + \max(0{,}20\log\left(\frac{H_m}{10}\right))$$

and,

$$b(H_b) = \min\,(0{,}20\log\left(\frac{H_b}{30}\right)).$$

Case 1: $d \leq 0.04\ km$

$$L = 32.4 + 20\log(f) + 10\log\left(d^2 + \frac{(H_B + H_M)^2}{10^6}\right) \tag{8}$$

Case 2: $d \geq 0.1\ km$

Sub-Case 1: Urban

$$L = 46.3 + 33.9\log(f) - 13.82\log(\max(30, H_B)) + 44.9 - 6.55\log(\max(30, H_B))\log(\mathrm{d}) - a(H_M) - b(H_b) \tag{9}$$

Sub-Case 2:

$$L = L(Urban) - 2\log\left(\frac{f}{28}\right)^2 - 5.4 \tag{10}$$

Sub-Case 3:

$$L = L(Urban) - 4.78(\log(f))^2 + 18.33\log(f) - 49.94 \tag{11}$$

Case 3: $0.04km < d < 0.1\ km$

$$L = L(0.04) + \frac{\log(d) - \log(0.04)}{\log(0.1) - \log(0.04)}\big(L(0.1) - L(0.04)\big) \tag{12}$$

For this research, when applying the Extended Hata-Model the frequency f was set to 1775 MHz and d was varied depending on the cell tower radii calculated using the ball tree algorithm.

Limitations

Of the models used in this research, Extended Hata-Okumura provides the most useful results. However, Extended Hata-Okumura is limited to three morphologies (i.e., urban, suburban, rural) and cannot take into account new morphologies from NLCD.

Conclusion

The Extended Hata-Okumura model is based on drive testing and includes rural, suburban, and urban clutter categories. With extensions into higher frequencies and sub-1 km applications, Extended Hata-Okumura provides more realistic propagation predictions for this research.

Free Space and Extended Hata-Okumura Propagation Model Results

This section presents the results of the path loss values when using the free-space and Extended Hata-Okumura models. These results should also give the reader valuable insight on how estimating ground cover using Census data versus NLCD data significantly affects the calculations of path loss. To understand how the path loss distributions differ between the two ground cover estimation methods, the researchers applied the Mann-Whitney test. The Mann-Whitney statistical test computes the probability that a set of samples $x_i \in$

$X\ and\ y_i \in Y$ are sampled from the same probability distribution. Computing the difference between the probability distributions gives insight into the extent to which the Census methodology and NLCD methodology affect the calculation of path loss distributions. This research tested the following set of hypotheses:

$H_0: X = Y$

$H_a: X \neq Y$

Significance Level: $\alpha = 0.05$,

where H_0 and H_a are the null and alternative hypotheses respectively, and X and Y are the path loss distributions from the Census and NLCD methodologies. For each Mann-Whitney test the researchers reported the derived p-value and .95 confidence interval.

Analysis for both Free Space and Extended Hata-Okumura begins with the cell radii calculated for each morphology (i.e., urban, suburban, rural). Table 5 shows the results.

Table 5. Mean Cell Radii Using the Ball Tree Algorithm

	Cell Radii Mean (km)		
Type	**Rural**	**Suburban**	**Urban**
Census Data	8.52	3.34	1.6
NLCD	3.16	1.73	1.03

Free Space Results

From the cell radii and path loss data, the researchers calculated path loss distributions for each morphology; the results are shown in Figure 11 and Figure 12 should the median path loss value for each is shown in Table 6. The figures show that the path loss distributions vary a significant amount. Using the NLCD methodology mentioned earlier, the NLCD data causes what the researchers describe as "information loss." For the purposes of this paper, the researchers defined "information loss" as towers that were originally labeled as urban, suburban, and rural in the Census data and with the free space model are labeled as dense urban, rural forested, barren, or suburban forested. Table 7 and Table 8 show that a large portion of the data has been lost to the additional NLCD categories of dense urban, rural forested, barren, or suburban forested.

Table 6. Median Free Space Path Loss for Each Morphology by Cell Tower Data Set

	Median (dB)		
Path Loss Function	**Rural**	**Suburban**	**Urban**
Census Free Space	115	104	100
NLCD Free Space	105	96	95

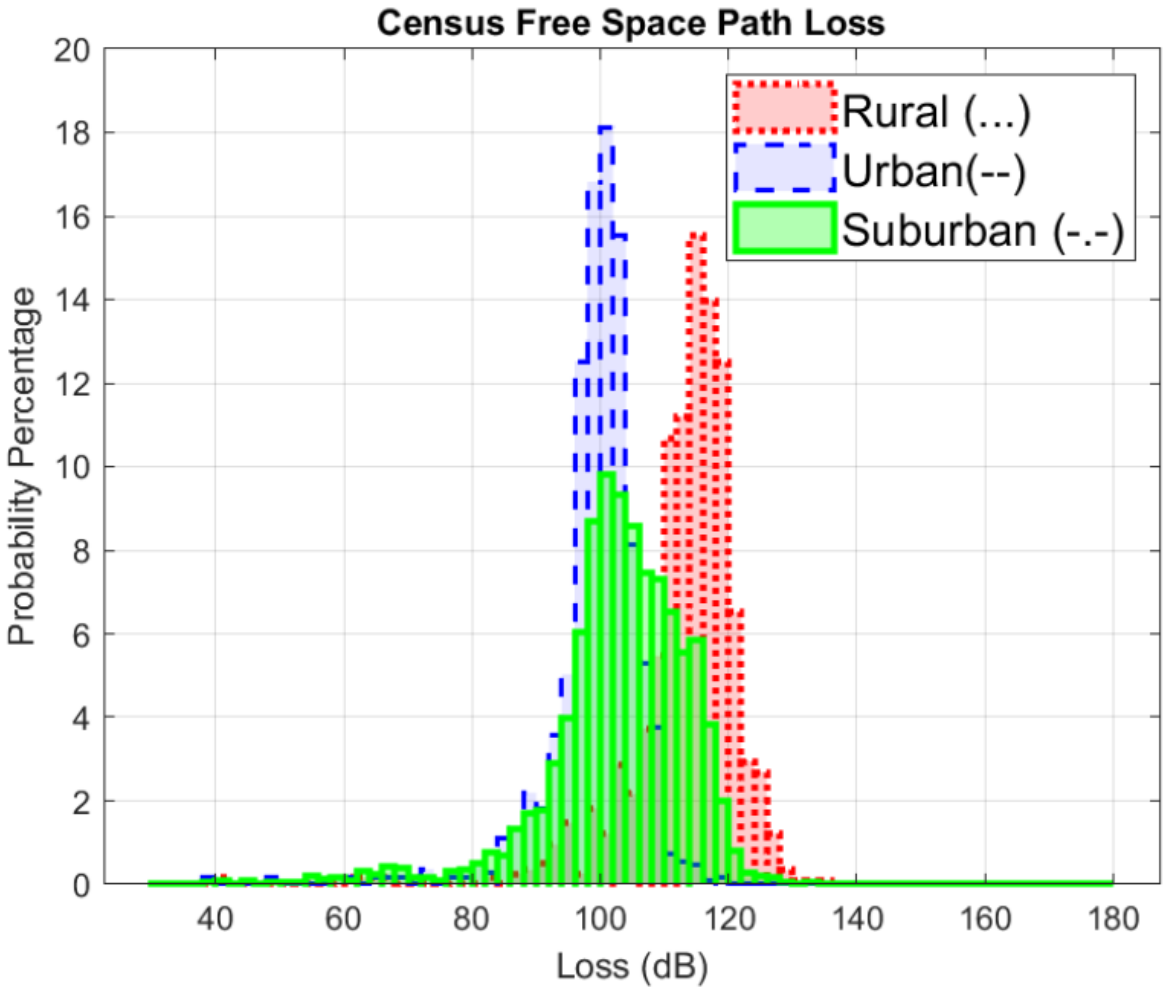

Figure 11. Census-based Free Space Path Loss Distributions

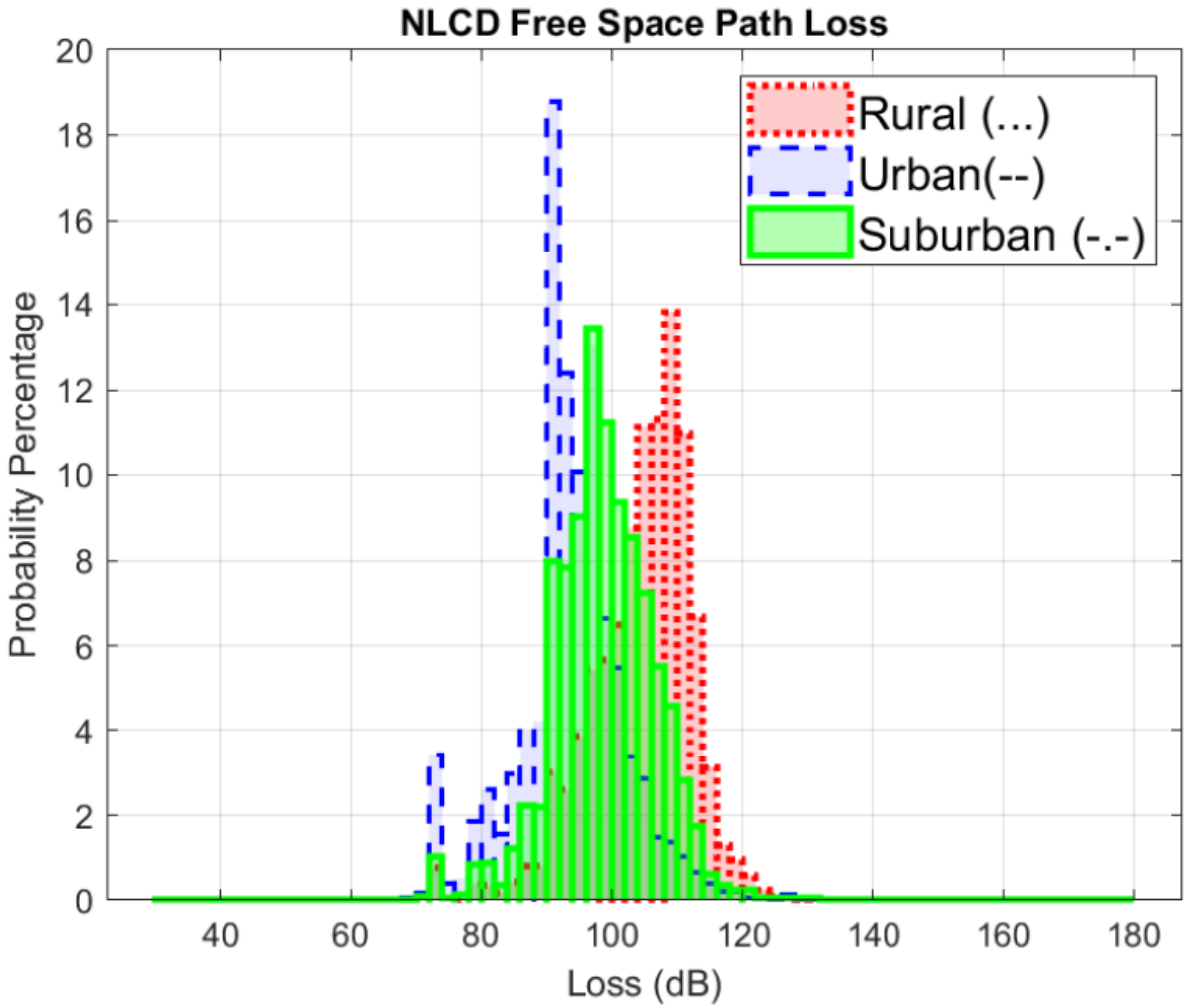

Figure 12. NLCD-based Free Space Path Loss Distributions

Table 7 clearly shows this "information loss." The reader should note that a significant amount of areas that were labeled as urban in the Census data have been distributed into the other six morphologies. Further, the tower counts for the Census-based methodology do not add up to the total 14,038 towers found in the provider data set because some towers in the provider data set are not in the ZCTA dataset. The section below on Corrective Approaches outlines the researchers' attempt to apply corrective measures against this "information loss" in order to avoid comparing two significantly disproportionate population counts. Table 8 shows the bin counts and mean cell-radius calculations for the seven morphologies when using the NLCD data method. Note that the total number of towers is 14,038, which is equal to the total number of towers in the provider data set. Even if a suitable approach is created to account for the increased NLCD morphologies, the research, to date has not found an acceptable propagation model to calculate path loss that accounts for the additional morphologies (i.e., rural forested, dense urban, suburban forested, or barren).

Table 7. Tower Counts for Rural, Suburban and Urban Using Census and NLCD Data

	Census Based	NLCD Based

Morphology	Tower Counts	Tower Counts
Rural	1,152	2,329
Suburban	10,201	1,738
Urban	1,094	2,804
Total	12,460	6,871

Table 8. Number of Towers for Each Morphology and Median Radius Using NLCD-based Calculations

	NLCD	
Morphology	**Tower Counts**	**Cell Radius Mean (km)**
Rural	2,329	3.25
Rural Forested	1,968	1.81
Suburban	1,738	1.59
Urban	2,804	1.09
Dense Urban	1,863	0.93
Suburban Forested	3,266	3.09
Barren	70	2.30
Total	14,038	-

Extended Hata-Okumura Results

Figure 13 and Figure 14 depict the findings when calculating path loss using the Extended Hata-Okumura model. The median path loss values are provided in Table 9. The reader should note that the urban and suburban path loss distributions have changed locations in comparison to Figure 11 and Figure 12. Referring to Table 5, the cell radius values in rural areas are larger simply due to their spatial features. In rural areas cell towers are spread out much farther than in suburban and urban areas. Due to the way the ball tree algorithm calculates cell-radii this causes large values of r for rural areas. As $r \to \infty$ in the free space equation, path loss values are larger, thus the change in distribution locations.

Table 9. Median Modified Hata Path Loss for Each Morphology by Cell Tower Data Set

	Median (dB)		
Path Loss Function	**Rural**	**Suburban**	**Urban**
Census Extended Hata-Okumura	129	136	145
NLCD Extended Hata-Okumura	115	125	135

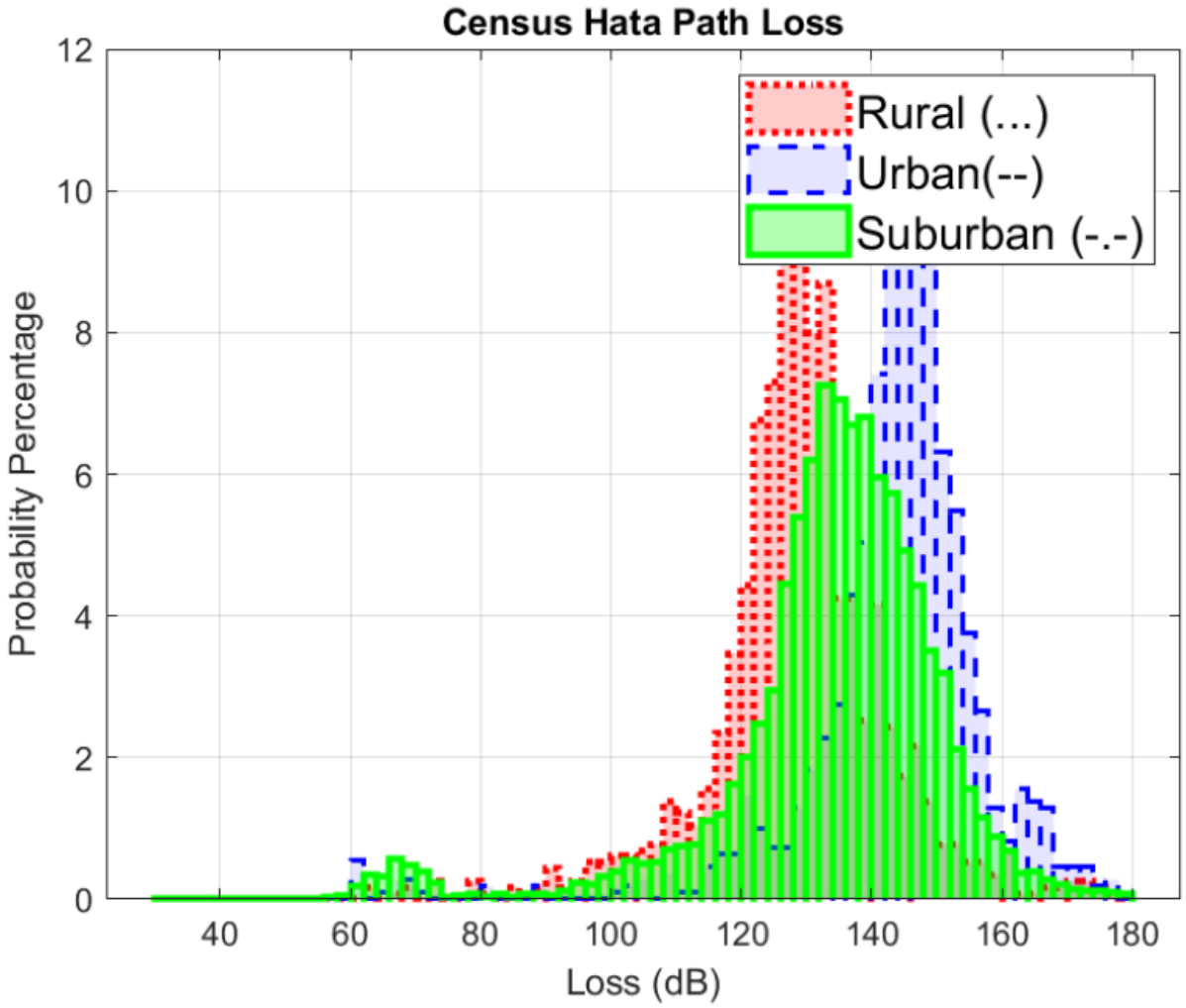

Figure 13. Census-based Hata-Okumura Model Path Loss Distributions

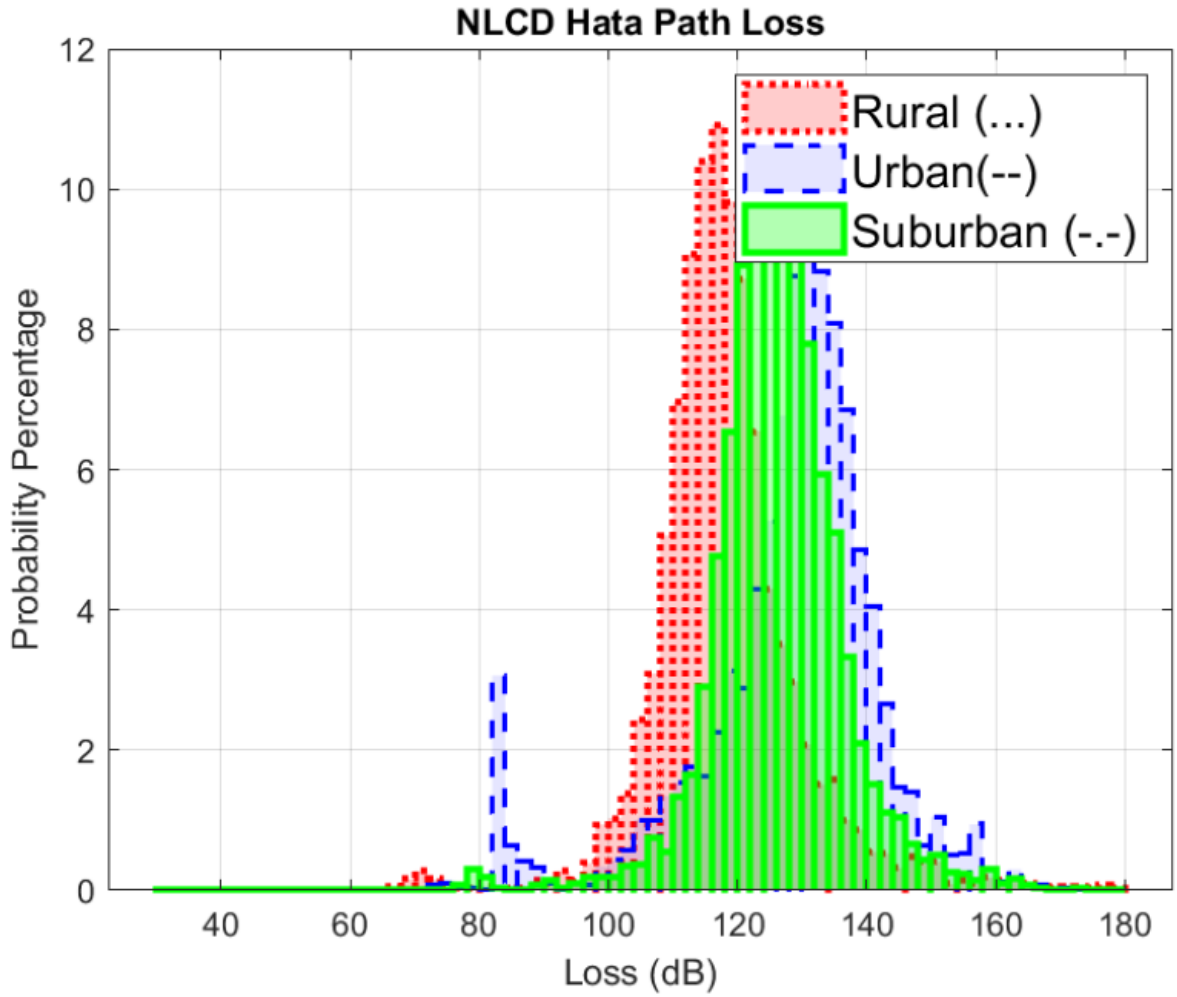

Figure 14. NLCD-based Hata-Okumura Model Path Loss Distributions

Since this research is primarily concerned with examining how land cover estimation affects path loss calculations the reader should focus on path loss outputs from the Extended Hata-Okumura model. The reader should also note that an 'apples to oranges' comparison occurs in relation to the sample sizes in the Census versus the NLCD data. Due to the nature of the Extended Hata-Okumura model, path loss calculations are possible only on the towers labeled with urban, suburban, and rural morphologies. Table 7 shows that the Census data contains 12,460 towers while the NLCD method, limited to the urban, suburban, and rural morphologies, contains only 6,871 towers. The next section describes a simple method to work around this issue.

Corrective Approaches

As noted previously, certain limitations must be addressed when estimating path loss using the Census data versus NLCD data: first, that the Extended Hata-Okumura model only considers path calculations for three morphologies (i.e., urban, suburban, and rural), and second, that a method is needed for appending the proper morphology to each cell tower in the data set. As shown, the NLCD estimation method can lose data when a tower is not included in the set of provided ZCTA data and that entire ZCTA will receive a certain

morphology based solely on the Census block count. To maintain the set of morphologies applied in the Extended Hata-Okumura model the researchers re-labeled the NLCD categories of dense urban, rural forested, suburban forested, and barren to their seemingly logical morphologies of urban, suburban, or rural. For the purposes of this research, the relabeling of the additional NLCD categories was:

- dense urban → urban
- suburban forested → suburban
- rural forested, barren → rural.

This relabeling allows the calculations to be performed on all available data for the Census and NLCD data categorizations. Table 10 shows the updated tower count using the relabeling technique. Figure 15 and Figure 16 show the results with the relabeling of NLCD categories to include all towers. It is noteworthy that in Table 11 and Table 12 the median path losses between NLCD Extended Hata-Okumura and NLCD Extended Hata-Okumura Re-labeled have not significantly changed due to a large number of samples being added their respective morphology. Because the results compare sample sizes that include the maximum amount of information that each method can accommodate, the researchers could perform the statistical tests mentioned earlier.

Table 10. Tower Counts for Each Morphology and Morphology Type

	Census Based	**NLCD Based**	**NLCD Relabeling**
Morphology	**Tower Counts**	**Tower Counts**	**Tower Counts**
Rural	1,152	2,329	4,367
Suburban	10,201	1,738	5,004
Urban	1,094	2,804	4,667
Total	12,460	6,871	14,038

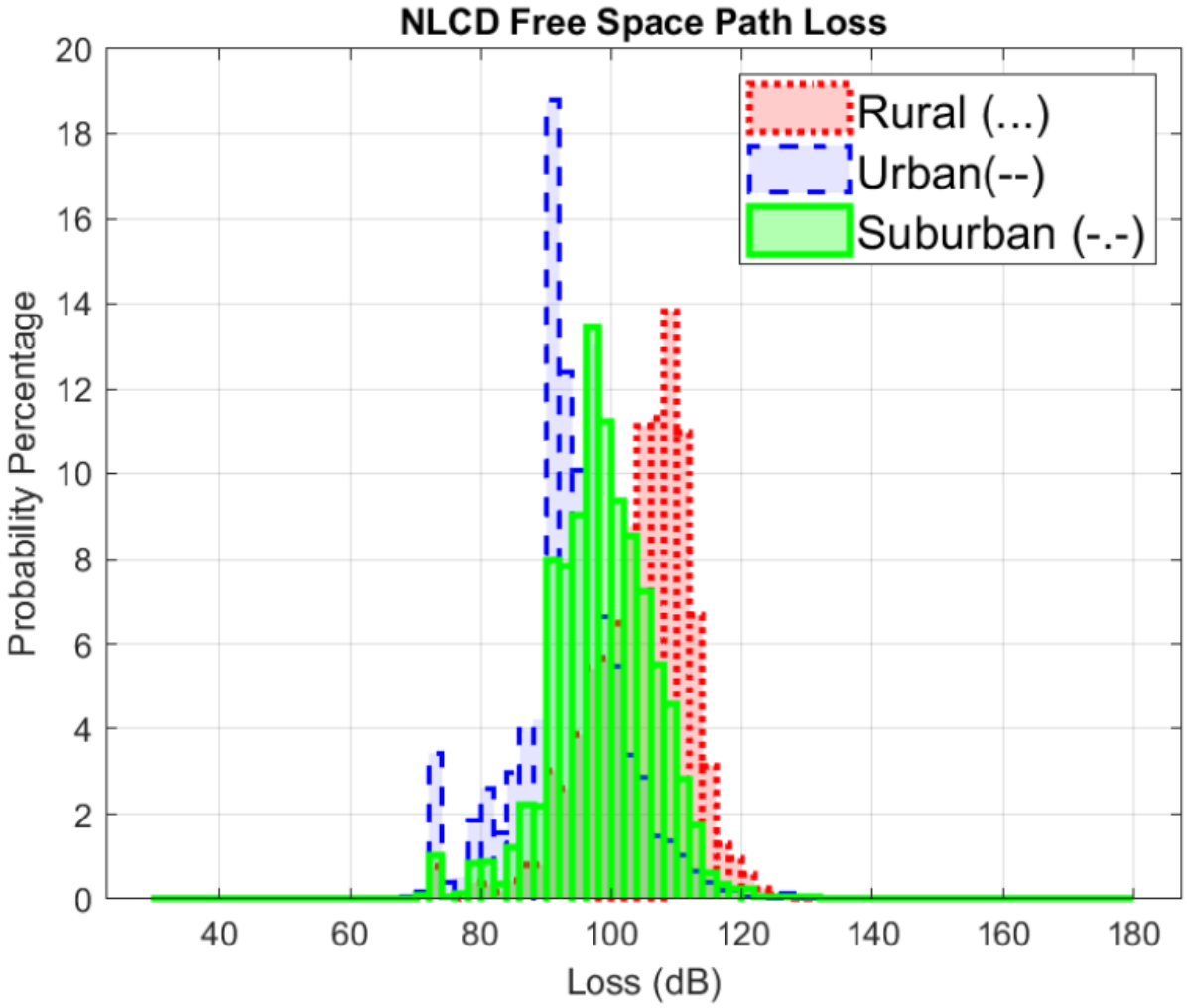

Figure 15. NLCD-based Free Space Model Path Loss Distributions with Re-labeled Morphologies

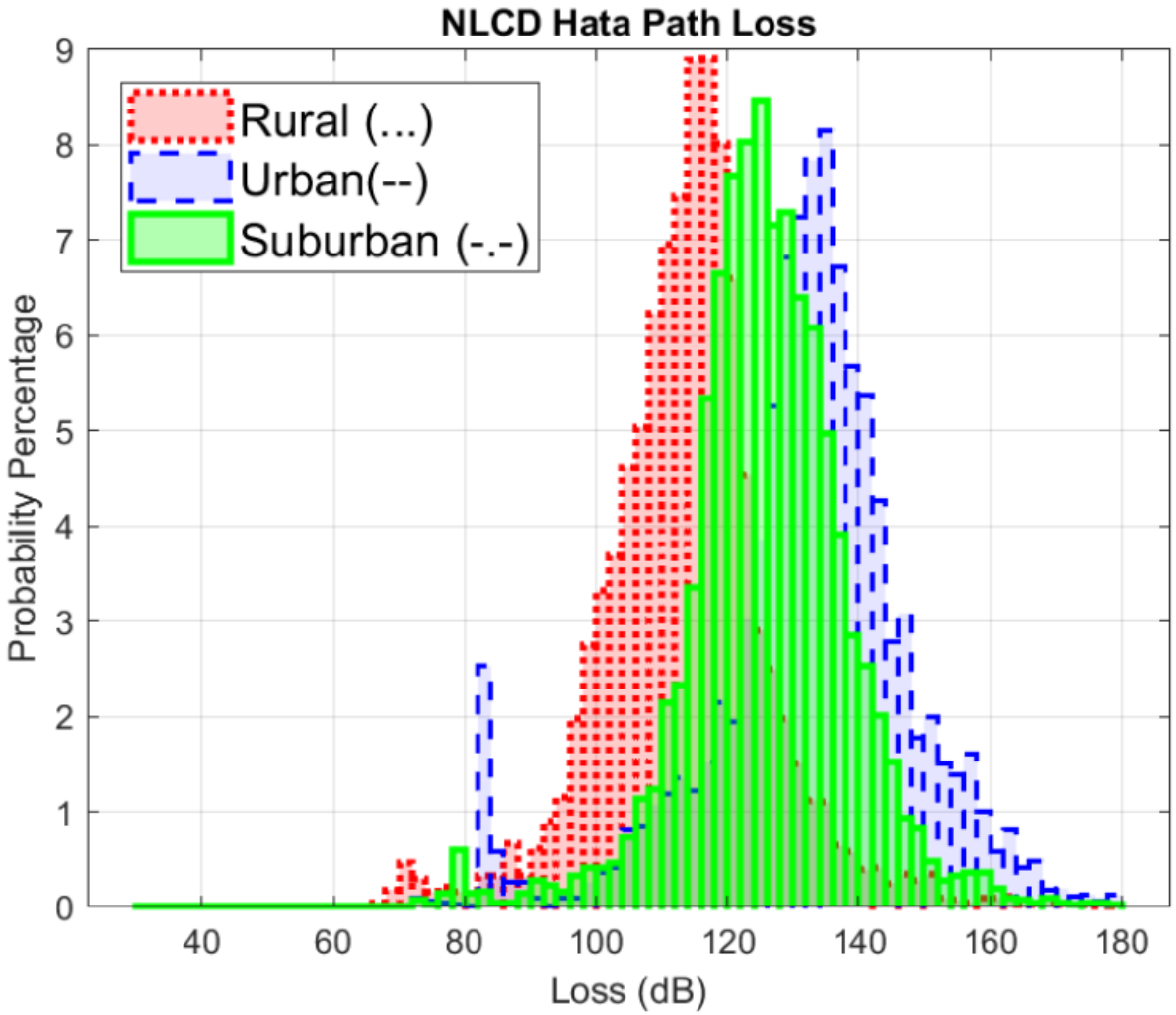

Figure 16. NLCD-based Extended Hata-Okumura Model Path Loss Distributions with Re-labeled Morphologies

Table 11. Median Free Space Path Loss for Each Morphology and Morphology Type

	Free Space Median (dB)		
Path Loss Function	**Rural**	**Suburban**	**Urban**
Census Free Space	115	107	100
NLCD Free Space	105	97	95
NLCD Free Space Relabeled	106	99	94

Table 12. Median Modified Hata Path Loss for Each Morphology and Morphology Type

	Hata Median (dB)		
Path Loss Function	**Rural**	**Suburban**	**Urban**
Census Hata	129	136	145
NLCD Hata	115	125	135
NLCD Hata Relabeled	117	126	130

The results in Table 13 show the p-value calculated was so small that the researchers could reject the null hypothesis H_0 in favor of the alternative hypothesis H_a and conclude that the path loss values sampled do not come from the same distribution. As shown in the table, p-value was significantly smaller than .05. To support this finding, Figure 17 shows a box-and-whisker plot of the path loss distributions, and it is seen that the median between the two path loss distributions is significantly different. This implies that that there is indeed a difference in distribution location when comparing rural path loss distributions between the Census and NLCD methodologies. In the figure, outliers are highlighted as red plus symbols.

Table 13. p-value for Census and NLCD Data for the Rural Morphology

	Census Rural vs. NLCD Rural
p-Value	$p < 0.05$
Confidence Interval	(-12, -11)

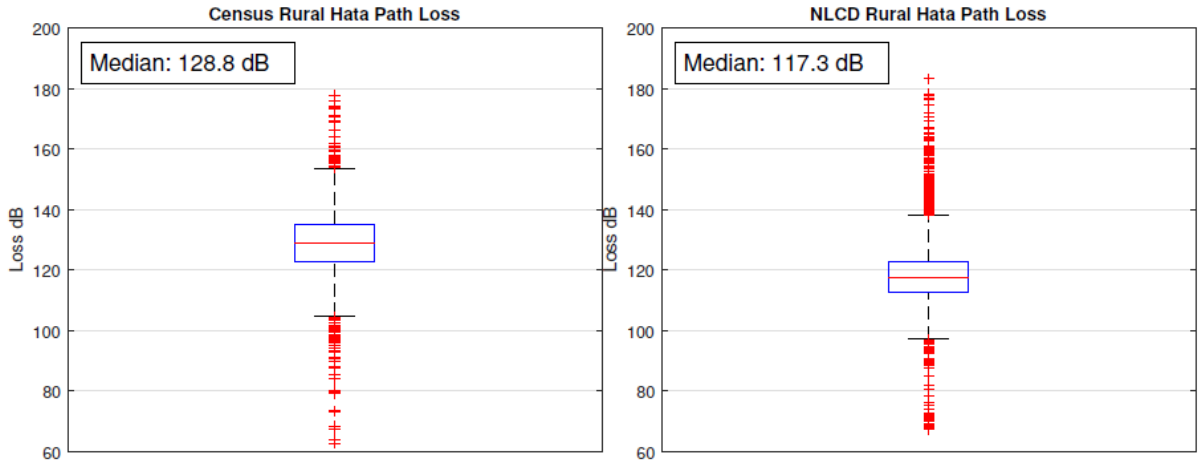

Figure 17. Box-and-Whisker Comparison of the Census and NLCD Morphology Methods for Rural

Table 14 shows the p-value computed for the suburban morphology, which is significantly smaller than .05. From this, the researchers could reject the null hypothesis H_0 in favor of the alternative hypothesis H_a and concluded that the path loss values sampled do not come

from the same distribution. To support this finding, Figure 18 shows a box-and-whisker plot of the path loss distributions; and it is seen that the median between the two path loss distributions is significantly different. This implies that that there is indeed a difference in distribution location when comparing suburban path loss distributions between the Census and NLCD methodologies. In the figure, outliers are highlighted as red plus symbols.

Table 14. p-value for Census and NLCD Data for the Suburban Morphology

	Census Suburban vs. NLCD Suburban
p-Value	$p < 0.05$
Confidence Interval	(-10, -9)

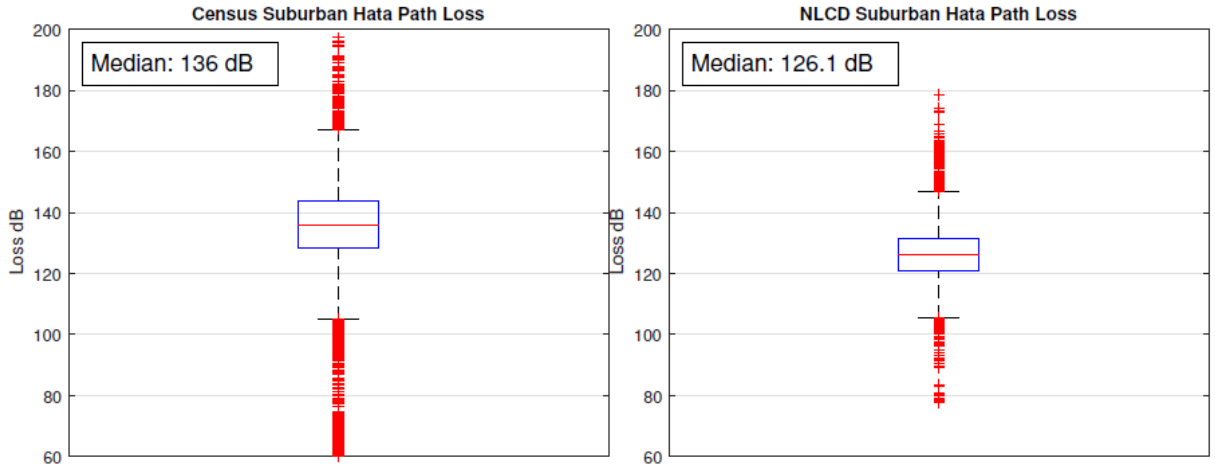

Figure 18. Box-and-Whisker Comparison of the Census and NLCD Morphology Methods for Suburban

Finally, Table 15 shows the p-value computed for the urban morphology, which is significantly smaller than .05. From this result, the researchers could reject the null hypothesis H_0 in favor of the alternative hypothesis H_a and concluded that the path loss values sampled do not come from the same distribution. To support this finding, Figure 19 shows a box-and-whisker plot of the path loss distributions; it is seen that the median between the two path loss distributions is significantly different. This implies that that there is indeed a difference in distribution location when comparing urban path loss distributions between the Census and NLCD methodologies. In the figure, outliers are highlighted as red plus symbols.

Table 15. p-value for Census and NLCD Data for the Urban Morphology

	Census Urban vs. NLCD Urban
p-Value	$p < 0.05$
Confidence Interval	(-16, -14)

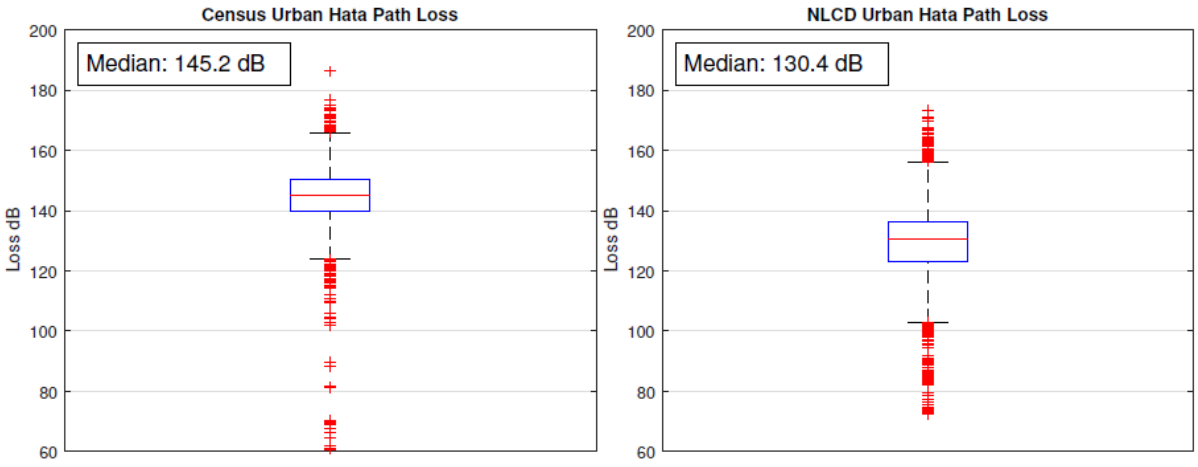

Figure 19. Box-and-Whisker Comparison of the Census and NLCD Morphology Methods for Urban Morphology

Areas for Future Research

This section outlines additional research that could benefit the accurate calculation of LTE path loss.

Other Propagation Models

This research implemented Friis's free space model, the Hata-Okumura model, and the Extended Hata-Okumura model. Since the research focused on how terrain estimation effects path loss calculations, future research could explore other terrain-based propagation models to determine if they could be of use to improve the accuracy of path loss predictions. Phillips et al. [17] examined a significant number of wireless path loss prediction models. However, only five of those models fall into what they categorize as "Terrain" models: the Edwards-Durkin, Allsbrook-Parsons, Blomquist-Ladell, Longley-Rice Irregular Terrain Model (ITM), and lastly the ITU-R 452 and ITU terrain models. Of those five models, the Longley-Rice Irregular Terrain Model and ITU-R 452 model appear to be of most value to future studies.

The DSO-sponsored spectrum sharing test and demonstration (SSTD) propagation tiger team identified the Winner II model as a 'model of choice' for most wireless carriers. Adding results from that propagation model may increase applicability of path loss estimates to commercial LTE stakeholders.

The following list identifies potential clutter-based propagation models for future study and includes brief descriptions.

- The Winner II channel model [18] is a geometrical and probabilistic model. It includes propagation scenarios for both indoor and outdoor scenarios (rural-macro cell, urban-macro cell, and suburban-macro cell).
- The Edwards-Durkin [17] model is an empirical model that was derived from measurements taken in the United Kingdom. The model is an additive model that sums free-space path loss with a correction from plane Earth propagation path loss.
- The Allsebrook-Parsons [17] model is an extension of the Edwards-Durkin model in that it sums additional path loss due to buildings. Empirical measurements were taken in British cities.
- The Longley-Rice ITM [17] computes the summation of free space path loss with knife-edge diffractions, path loss from the curvature of the Earth, and tropospheric scattering.
- ITU-R 452: The P452 [19] makes path loss predictions based on the summations of Free-Space path loss with loss from knife-edge diffraction over terrain, loss from atmospheric gases, loss from tropospheric scattering, ducting, coupling, and layer reflection in the atmosphere, loss due to the curvature of the Earth, and path loss from clutter using several morphologies outside of the commonly found rural, urban, and suburban morphologies.
- ITU terrain: The ITU terrain [17] model combines classical Free-Space path loss with a single diffraction due to terrain path loss. A Digital Elevation Model is used to compute the path loss from the most significant obstruction in the signals path.

- Blomquist-Ladell: The Blomquist-Ladell model [17] is similar to the Edwards-Durkin model in that it computes plane Earth propagation path loss with a correction factor and sums that with Free-Space path loss. This model was derived over "rolling" terrain in Sweden.

Validation with Real-world Measurements

Drive test data provides better insight into path loss distributions for the new set of morphologies generated by this study. Although making path loss calculations using empirically based (e.g., Extended Hata-Okumura model) models has merit, without having live data to compare to the model results against the researchers cannot validate their findings. Drive test measurements could also provide insight into cell radius estimation for the urban, dense urban, rural, rural forested, suburban, suburban forested, and barren area morphologies.

Other Related Work

Continuing to study this material is vital not only within the DSO and Department of Defense (DoD) mission space but also to the signal propagation community. Propagation models should be updated from the basic set of morphologies (rural, suburban, and urban) to expanded morphologies such as those presented in the NLCD (i.e., dense urban, urban, suburban, forested suburban, rural, rural forested, and barren). Future research should not only derive a new set of morphologies but should also take a set of measurements to potentially derive a set of empirical models.

Summary and Conclusion

This research developed and described a methodology to allow the determination of LTE path loss from a variety of tower datasets, land use morphologies, and propagation models. The NASCTN test team will use the data from this research to support the NASCTN project investigating the factors and sensitivities of UE behavior for the DSO.

The research has shown that the morphology and propagation model used significantly affects the path loss distributions for a set of morphologies. For the rural, suburban, and urban morphologies the Mann-Whitney Test showed a difference in distribution location when comparing the Census-based and NLCD-based propagation models. These findings are of significant value to the NASCTN testbed, as they provide information on realistic cell radii and/or propagation loss for multiple morphologies for test execution, which in turn improves the utility of the results for the DSO.

This research and methodology have potential applicability and utility to other LTE-related research by the DSO and other federal and commercial stakeholders. This research, however, represents just one step. This paper identified several areas for additional research and improvements.

The ground cover data, categorization morphologies, and cell tower radii significantly affect results. Ground cover changes over time, resulting in regular updates to the NLCD. Additionally, research continues into improving the resolution, algorithms, and categorization of ground cover data. Location of cell towers also changes over time and requires periodic updates to accurately reflect changes in cell radii and impact by land use morphologies. Therefore, this methodology should be repeated regularly as updates to the NLCD and cell tower location become available.

The propagation model chosen to calculate path loss has a major effect on results. The propagation models used in this study limit the number of morphologies that can be modeled. This research concludes that further insight into the validity of the methodologies and calculations is possible from the use of more rigorous propagation models than the free-space and Extended Hata-Okumura models. This is not to say that the models have no value; however, obtaining a better understanding of the expected path loss for an expanded and more granular set of morphologies (e.g., urban, dense urban, suburban, suburban forested, rural, rural forested and barren) requires different propagation models.

References

[1] American Tower, "American tower locations." [Online]. Available: http://www.americantower.com/corporateus/articles/find-sites.htm

[2] Unwired Labs, "Open cell id project." [Online]. Available: https://www.opencellid.org/downloads.php

[3] Statistic Brain Research Institute, "Cell phone tower statistics." [Online]. Available: https://www.statisticbrain.com/cell-phone-tower-statistics/

[4] H. T. Friis, "A note on a simple transmission formula," in *Proceedings of the Institute of Radio Engineers*, vol. 34, no. 5, 1946, pp. 254–256.

[5] CSMAC, "Commerce spectrum management advisory committee (csmac) working group 3 (wg3) report on 1755-1850 MHz satellite control and electronic warfare," 2013. [Online]. Available: https://www.ntia.doc.gov/files/ntia/Working_Group_3_Final.pdf/

[6] SkLearn Developers, "Balltree for fast generalized n-point problems." [Online]. Available: https://scikit-learn.org/stable/modules/generated/sklearn.neighbors.BallTree.html

[7] Marianne , "Lost but lovely: The haversine," *Plus Magazine*, 2014. [Online]. Available: https://plus.maths.org/content/lost-lovely-haversine

[8] K. Weinberger, "Lecture 16- kd trees," Cornell Lecture Notes, 2015. [Online]. Available: http://www.cs.cornell.edu/courses/cs4780/2015fa/web/lecturenotes/lecturenote16.html

[9] SciKit-Learn Developers, "Nearest neighbors." [Online]. Available: https://scikit-learn.org/stable/modules/neighbors.html

[10] United States Census Bureau, "Zip codeTM tabulation areas (zctasTM)," 2010. [Online]. Available: https://www.census.gov/geo/reference/zctas.html

[11] —, "Explanation of the 2010 urban area to ZIP code tabulation area (ZCTA) relationship file," 2010. [Online]. Available: https://www2.census.gov/geo/pdfs/maps-data/data/rel/explanation_ua_zta_rel_10.pdf

[12] L. Yand et al., "A new generation of the United States national land cover database: Requirements, research priorities, design, and implementation strategies," *ISPRS Journal of Photogrammetry and Remote Sensing*, vol.146, pp. 108–123, 2018.

[13] Multi-Resolution Land Characteristics Consortium, "NLCD Data." [Online]. Available: https://www.mrlc.gov/data

[14] C. H. Homer, J. A. Fry, and C. A Barnes, "The national land cover database," U.S. Geological Survey, Tech. Rep. 2012. [Online]. Available: https://pubs.usgs.gov/fs/2012/3020/

[15] Multi-Resolution Land Characteristics Consortium, “NLCD Legend of Pixel Values.” [Online]. Available: https://www.mrlc.gov/sites/default/files/NLCD_Colour_Classification_Update.jpg

[16] A. F. Molisch, *Wireless Communications*. John Wiley and Sons, 2005. [Online]. Available: https://www.wiley.com/legacy/wileychi/molisch/supp2/appendices/c07_Appendices.pdf

[17] C. Phillips, D. Sicker, and D. Grunwald, “A survey of wireless path loss prediction and coverage mapping methods,” *IEEE Communications Surveys and Tutorials*, vol. 15, no. 1, pp. 255–270, 2013.

[18] Information Society Technologies, “Winner II Channel Models,” IST-4-027756 WINNER II, 2007. [Online]. Available: https://www.cept.org/files/8339/winner2%20-%20final%20report.pdf

[19] International Telecommunication Union, “Prediction procedure for the evaluation of interference between stations on the surface of the earth at frequencies above about 0.1 GHz,” ITU-R, P Series ITU-R P.452-16, 2015. [Online]. Available: https://www.itu.int/dms_pubrec/itu-r/rec/p/R-REC-P.452-16-201507-I!!PDF-E.pdf

Abbreviations and Acronyms

3G	3rd Generation
3GPP	3rd Generation Partnership Project
4G	4th Generation
API	Application Program Interface
AWS-3	Advanced Wireless Services 3
CDMA	Code Division Multiple Access
CONUS	Continental United States
CSMAC	Commerce Spectrum Management and Advisory Committee
CSV	Comma-Separated Values
dB	Decibel
DEM	Digital Elevation Model
DISA	Defense Information Systems Agency
DoD	Department of Defense
DSO	Defense Spectrum Organization
DUT	Device Under Test – User Equipment
eNB	Evolved Node B
GSM	Global System for Mobile Communications
ICIC	Inter-Cell Interference Coordination
IP	Internet Protocol
ITU	International Telecommunications Union
km	Kilometer
LTE	Long-Term Evolution
m	Meter
MIMO	Multiple Input-Multiple Output
NASCTN	National Advanced Spectrum and Communications Test Network
NLCD	National Land Cover Database
RF	Radio Frequency
SSTD	Spectrum Sharing Test and Demonstration
TRP	Total Radiated Power
UE	User Equipment
UMTS	Universal Mobile Telecommunications System

USA	United States of America
UTG	User Equipment Traffic Generator
VoLTE	Voice over Long-Term Evolution
WG	Working Group
ZCTA	ZIP Code Tabulation Area